remote sensing

MDPI

Supplementary Materials

Prediction of Open Woodland Transpiration Incorporating Sun-Induced Chlorophyll Fluorescence and Vegetation Structure

Sicong Gao [1,2,*], William Woodgate [3], Xuanlong Ma [4] and Tanya M. Doody [1]

[1] CSIRO, Environment, Waite Campus, Adelaide, SA 5064, Australia
[2] Centre for Applied Water Science, University of Canberra, Canberra, ACT 2601, Australia
[3] Remote Sensing Research Centre, School of Earth and Environmental Sciences, The University of Queensland, Brisbane, QLD 4072, Australia
[4] College of Earth and Environmental Sciences, Lanzhou University, Lanzhou 730020, China
* Correspondence: steve.gao@csiro.au

Method Validation

The entire workflow was designed to retrieve canopy scale parameters for FluorFLiES model and simulate SIF for various bands. It is noted that fine scale SIF measurements in Australia floodplain are unavailable, for example, the best SIF satellite spatial resolution is 1 km and temporal resolution has a few days interval, so it is difficult to validate SIF satellite measurements with the fine-scale sap flow measurements of transpiration (30 minutes interval and 50 m^2 plot).

The workflow was evaluated using existing datasets, and validation parts include SIF model FluorFLiES, LAI partitioning, retrieved bioparameters using two-step inversion, and soil reflectance.

FluorFLiES has been validated with field measurements of SIF and its performance was compared with other SIF models [1]. The simulated SIF is able to quantify SIF measurements with good accuracy, $R^2 = 0.83$, and RMSE = 0.19 mW m^{-2} sr^{-1} nm^{-1} for mature forest.

Two-step inversion method has been applied to simulate SIF using a one-dimensional radiative transfer model [2]. This method has been proved to lead the accurate simulation of SIF. Relying on two-step inversion, FluorFLiES simulated SIF also compared with satellite SIF (TROPOMI in 1 km spatial resolution), the R^2 was 0.53 (Figure S5 in Supplementary Materials). Although satellite SIF spatial resolution is much coarse than model simulations, we found that they were correlated with each other at the seasonal scale.

LAI partitioning method has been validated with field measured LAI in Australia and has been applied to partition GPP and ET into tree and grass layers [3,4]. This method was validated in Australian woodlands, where vegetation cover is similar to our study sites. Partitioned tree LAI could explain 97% variations of the field measured canopy LAI, and their seasonal variations was highly correlated (Figure 3 in [3]).

Chlorophyll content (Cab) is the most important parameter among bioparameters (BP), which mainly contributes to the SIF emissions [5]. We validated retrieved Cab using a chlorophyll content index [6], which is a vegetation index indicating Cab variations. It was found that retrieved Cab was highly correlated with chlorophyll content index (**Error! Reference source not found.**) with $R^2 > 0.6$, except for MC_{BB_S}. Other BP variations contribute less to SIF emissions [5] and to our knowledge, no effective vegetation index could explain their variations.

The soil reflectance setting was referred to a soil database, ICRAF-ISRIC Soil VNIR Spectral Library (http://www.isric.org/data/icrafisric-spectral-library, accessed on 20 November 2023). We extracted soil spectral measurements in Australia and found that soil

reflectance was ranging from 0.1 to 0.5 from PAR to NIR region (**Error! Reference source not found.**). Soil reflectance retrievals based on two-step inversion was consistent with soil spectral measurements.

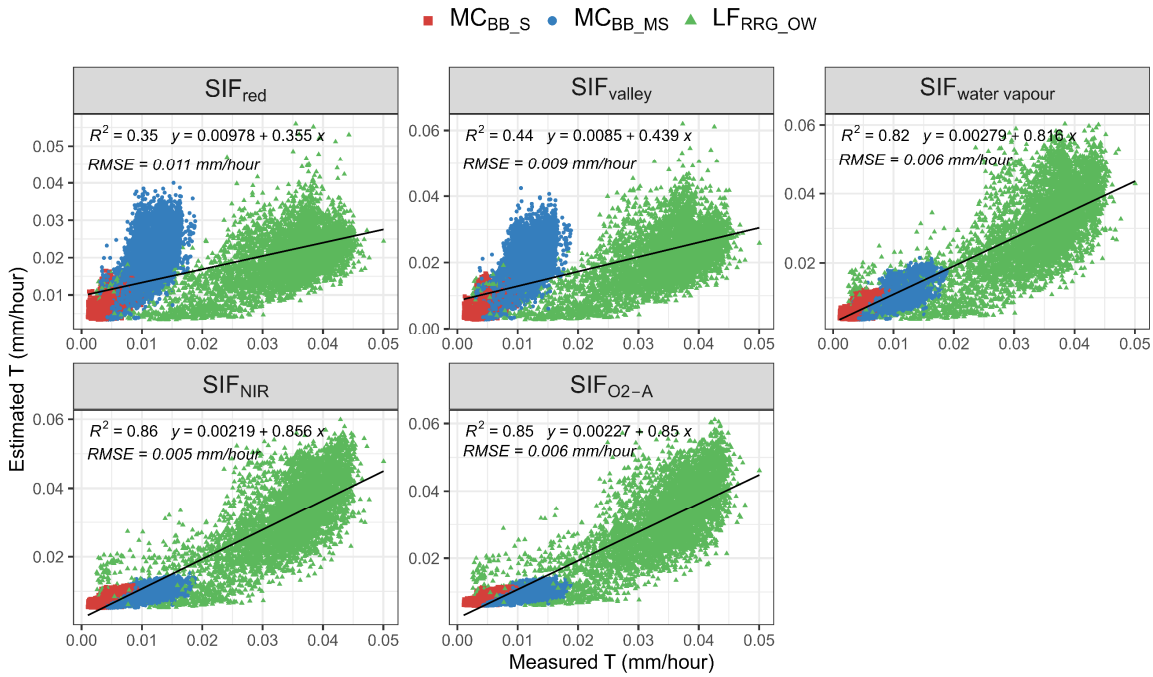

Figure S1. Scatter plot of estimation of transpiration (T) versus measured T for sun-induced chlorophyll fluorescence (SIF) emissions at 685 nm (SIF_{red}); 699 nm (SIF_{valley}); 720 nm ($SIF_{water\ vapour}$); 740 nm (SIF_{NIR}); 760 nm (SIF_{O2-A}) for Mallee Cliffs *E. largiflorens* sparse site (MC_{BB_S}), Mallee Cliffs *E. largiflorens* moderate-sparse site (MC_{BB_MS}) and Lindsay Forest *E. camaldulensis* open woodland site (LF_{RRG_OW}).

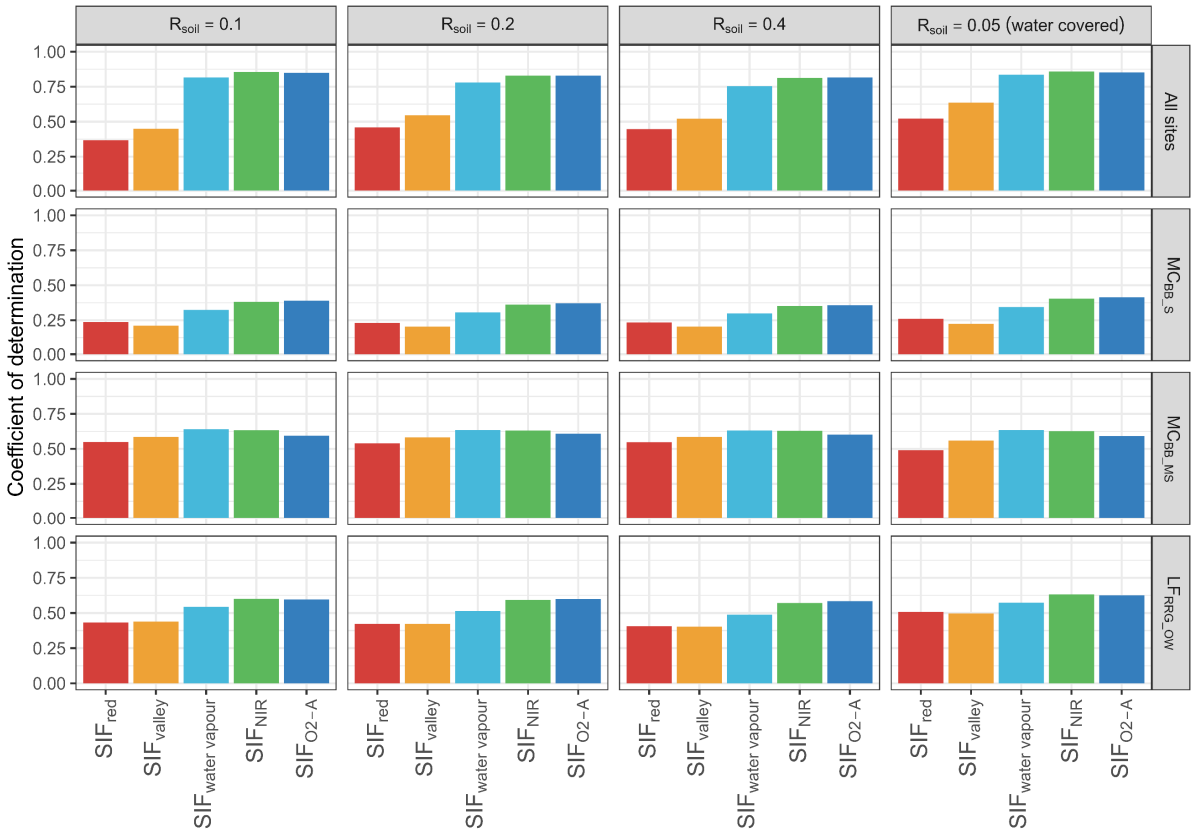

Figure S2. Coefficient of determinations of correlations between transpiration (T) and sun-induced chlorophyll fluorescence (SIF) emissions at hourly scale with defined soil reflectance (R_{soil}) for each site. MC_{BB_S} is Mallee Cliffs *E. largiflorens* sparse site, MC_{BB_MS} is Mallee Cliffs *E. largiflorens* moderate-sparse site and LF_{RRG_OW} is Lindsay Forest *E. camaldulensis* open woodland site. SIF_{red} is SIF emission at 685 nm; SIF_{valley} is 699 nm; $SIF_{water\ vapour}$ is 720 nm; SIF_{NIR} 740 nm; SIF_{O2-A} is 760 nm.

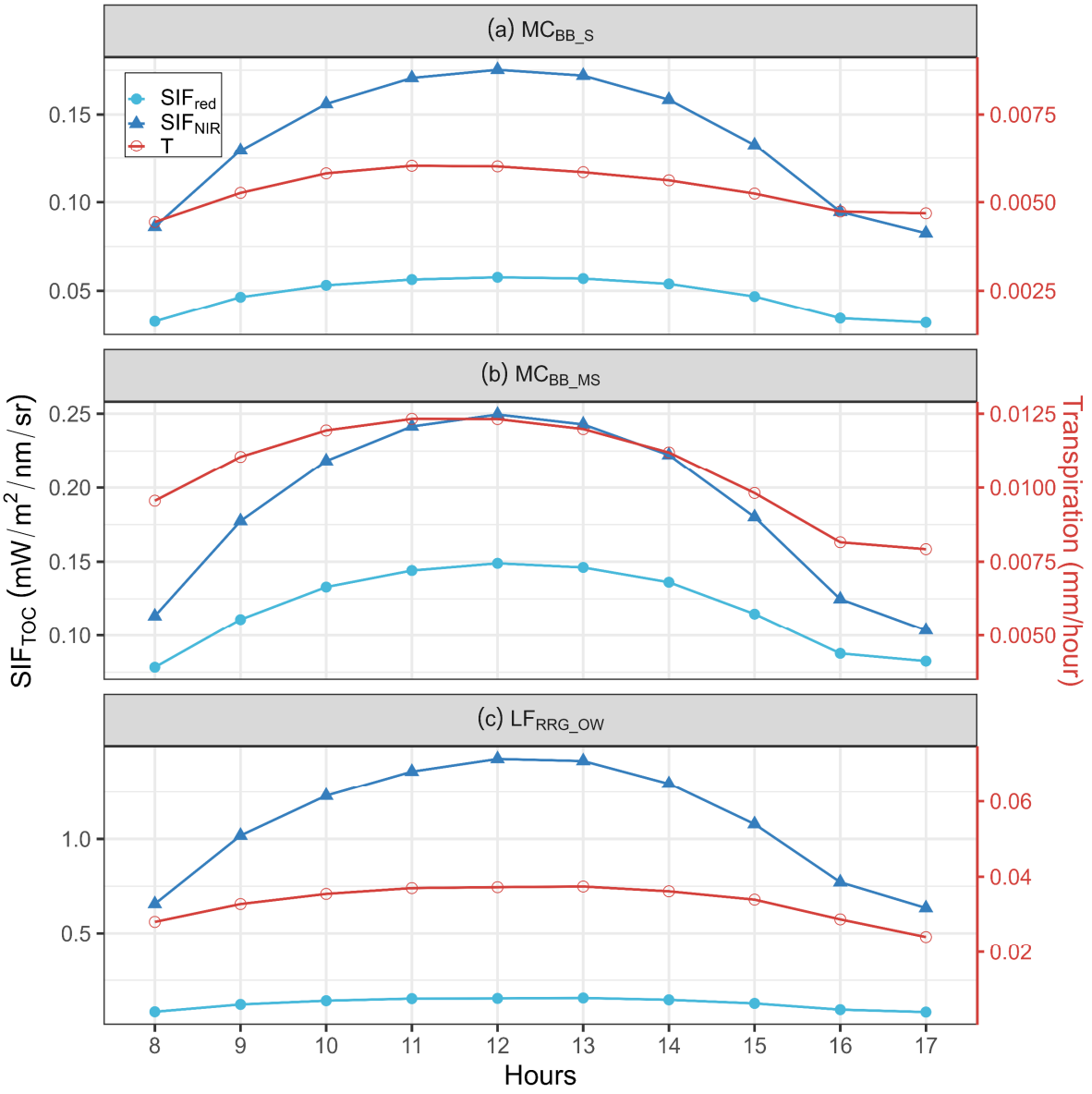

Figure S3. Mean diurnal patterns of sun-induced chlorophyll fluorescence (SIF) emission at 685 nm (SIF_{red}), SIF emission at 740 nm (SIF_{NIR}), and transpiration (T) for (a) Mallee Cliffs *E. largiflorens* sparse site (MC_{BB_S}), (b) Mallee Cliffs *E. largiflorens* moderate-sparse site (MC_{BB_MS}) and (c) Lindsay Forest *E. camaldulensis* open woodland site (LF_{RRG_OW}).

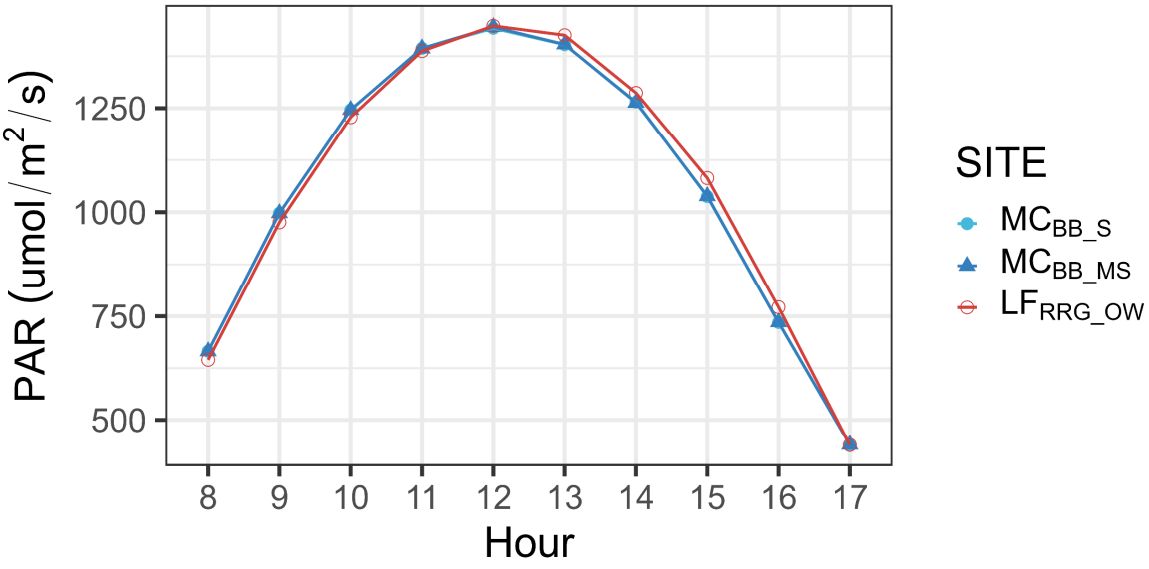

Figure S4. Diurnal photosynthetic active radiation for each site. MC_{BB_S} is Mallee Cliffs *E. largiflorens* sparse site, MC_{BB_MS} is Mallee Cliffs *E. largiflorens* moderate-sparse site and LF_{RRG_OW} is Lindsay Forest *E. camaldulensis* open woodland site.

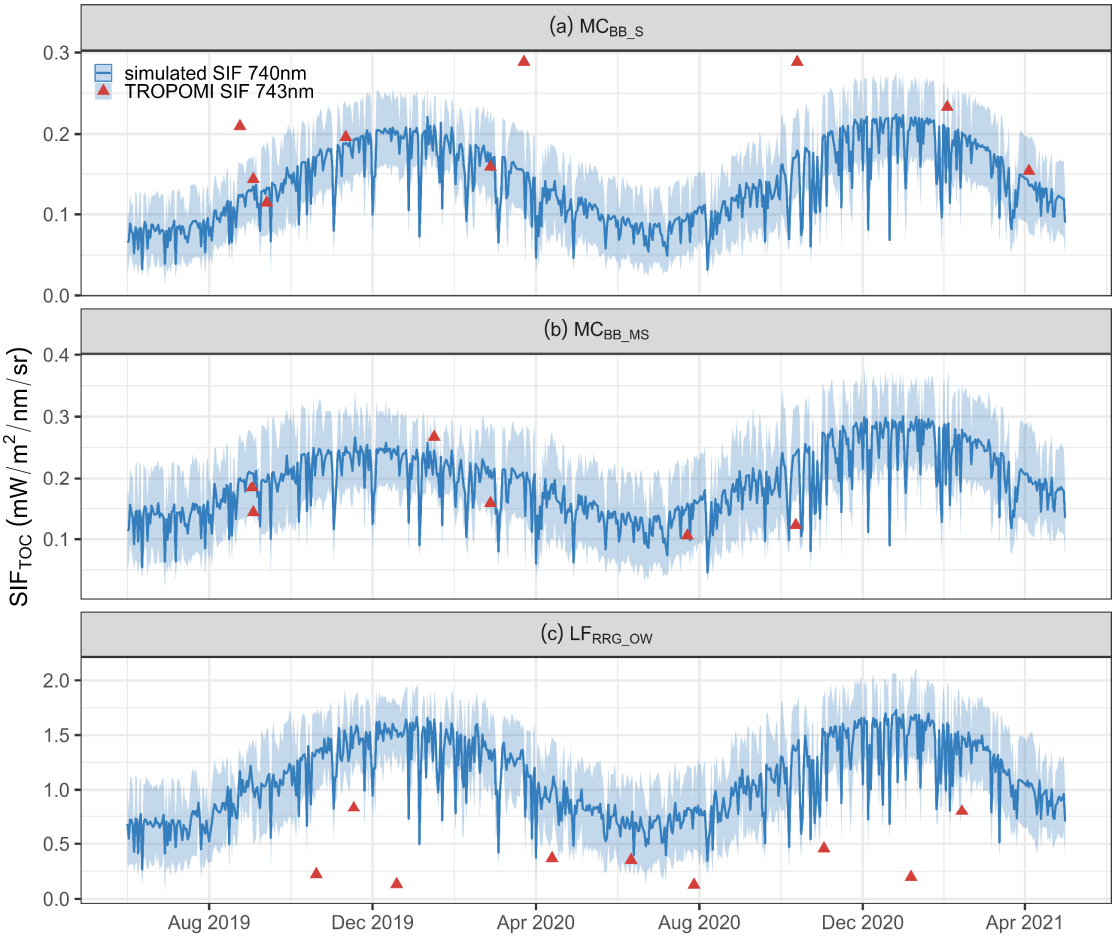

Figure S5. FluorFLiES model simulated SIF at 740 nm compared with TROPOMI SIF at 743 nm for (a) Mallee Cliffs *E. largiflorens* sparse site (MC_{BB_S}), (b) Mallee Cliffs *E. largiflorens* moderate-sparse site (MC_{BB_MS}) and (c) Lindsay Forest *Eucalyptus camaldulensis* open woodland site (LF_{RRG_OW}).

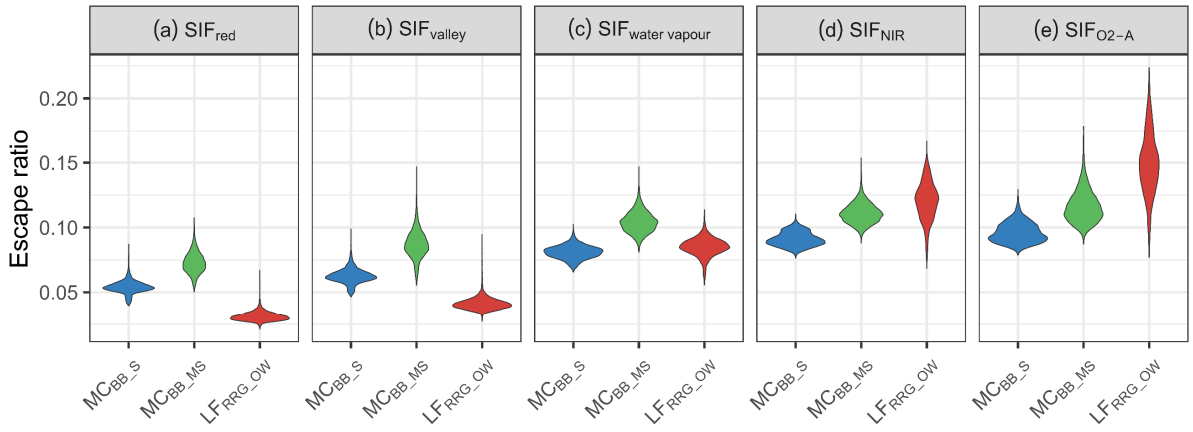

Figure S6. Violine plots of escape ratio of (a) sun-induced chlorophyll fluorescence (SIF) emission at 685 nm (SIF_{red}); (b) 699 nm (SIF_{valley}); (c) 720 nm ($SIF_{water\ vapour}$); (d) 740 nm (SIF_{NIR}); 760 nm (SIF_{O2-A}) for Mallee Cliffs *E. largiflorens* sparse site (MC_{BB_S}), Mallee Cliffs *E. largiflorens* moderate-sparse site (MC_{BB_MS}) and Lindsay Forest *E. camaldulensis* open woodland site (LF_{RRG_OW}).

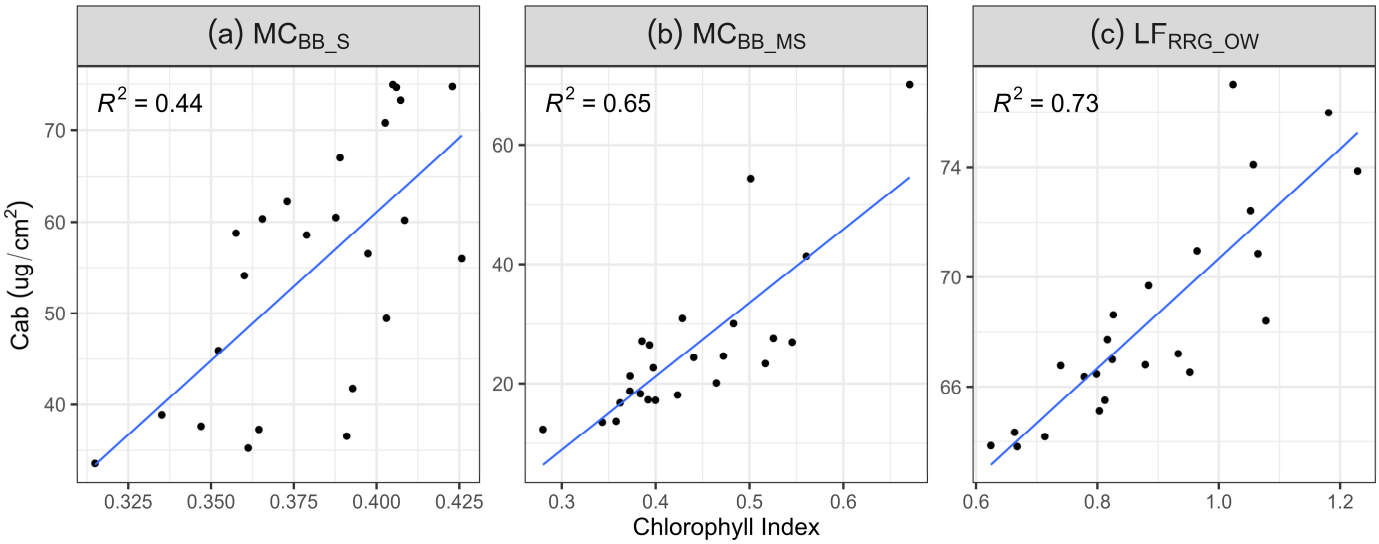

Figure S7. Correlations between retrieved chlorophyll content (Cab) and Chlorophyll index (retrieved from Sentinel-2).

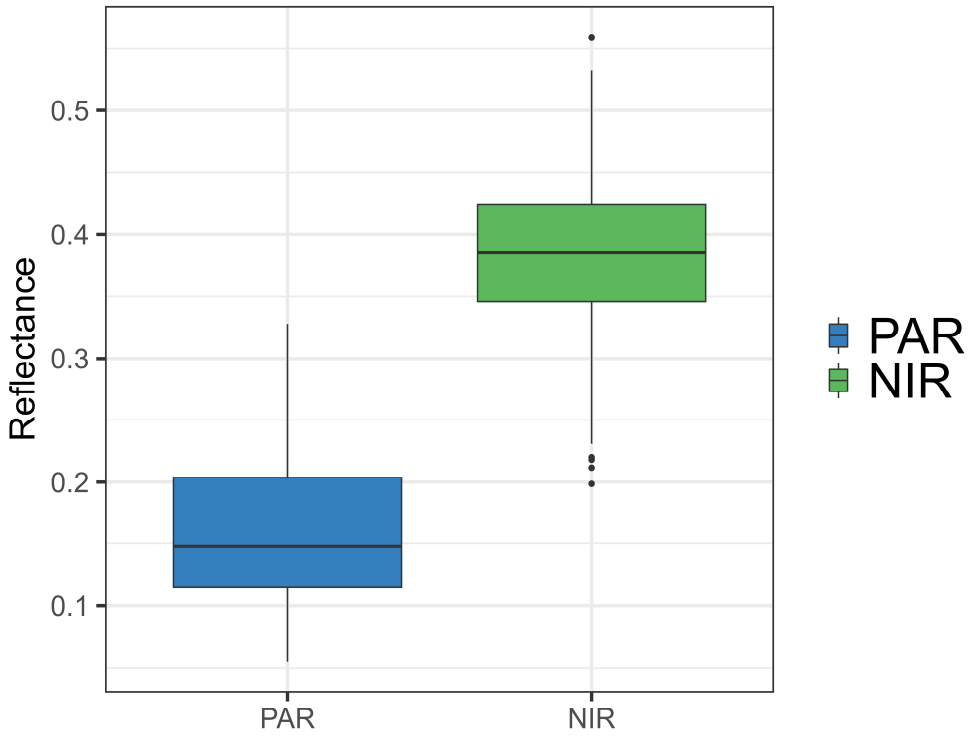

Figure S8. Soil reflectance value range from ICRAF-ISRIC Soil VNIR Spectral Library at PAR and NIR region, respectively.

Table S1. Full names of acronyms used in this study.

Acronym	**Full name**
1-D	one-dimensional
3-D	three-dimensional
BAD	Branch Area Density
BB	black box tree
BP	bioparameters
C_{ab}	leaf chlorophyll a+b content
C_{car}	total carotenoid content
C_{dm}	leaf dry matter content
C_s	senescence material
C_w	leaf water content
EF-matrix	excitation-fluorescence matrices
ET	evapotranspiration
EVI	enhanced vegetation index
FAPAR	fraction of absorbed photosynthetically active radiation
$FAPAR_F$	fraction of absorbed photosynthetically active radiation simulated by FLiES model
f_{esc}	fluorescence escape ratio
FLiES	Forest Light Environmental Simulator
FluorFLiES	Fluorescence Forest Light Environmental Simulator
FVC	fractional vegetation cover
$FVC_{product}$	a fractional vegetation cover product
GPP	gross primary production
H	height
LAD	leaf area density
LAD_F	leaf area density simulated by FLiES model

LAI	leaf area index
LAI_c	canopy leaf area index
LAI_F	leaf area index simulated by FLiES model
LAI_{S2}	Sentinel-2 leaf area index
LAI_u	understory leaf area index
LF_{RRG_OW}	Lindsay forest River Red Gum open woodland site
LUT	lookup table
LUT_{BP}	lookup table for retrieving bioparameter
LUT_{LAD}	lookup table for retrieving leaf area density
MC_{BB_S}	Mallee Cliffs Black Box sparse open woodland site
MC_{BB_MS}	Mallee Cliffs Black Box moderate-sparse open woodland site
MDB	Murray-Darling Basin
N	namely leaf mesophyll structure parameter
NDVI	normalized difference vegetation index
NIR	near-infrared
nm	nanometre
PAR	photosynthetically active radiation
P-M	Penman-Monteith
P-T	Priestley-Taylor
PSI	photosynthesis system I
PSII	photosynthesis system II
R	radius
ref	reflectance
RMSE	root Mean Square Error
RRG	river red gum
R_{soil}	soil reflectance
RTM	radiative transfer model
SAA	sun azimuth angle
SIF	sun-induced chlorophyll fluorescence
SIF_{canopy}	SIF monitored from canopy
SIF_{red}	SIF red band
SIF_{TOC}	SIF simulated at the top of canopy
SIF_{total}	total emitted SIF
SIF_{NIR}	SIF NIR band
$SIF_{O2\text{-}A}$	SIF O_2-A band
$SIF_{understory}$	SIF monitored from understory
$SIF_{water\ vapour}$	SIF water vapour band
SIF_{valley}	SIF valley band
SSA	singular Spectrum Analysis
SZA	sun zenith angle
T	transpiration
TEMP	temperature
tran	transpiration
TOC	top of canopy
VAA	viewing azimuth angle
VZA	viewing zenith angle
VI_F	FLiES simulated vegetation index
VI_{S2}	Sentinel-2 vegetation index

References

1. Gao, S.; Huete, A.; Kobayashi, H.; Doody, T.M.; Liu, W.; Wang, Y.; Zhang, Y.; Lu, X. Simulation of Solar-Induced Chlorophyll Fluorescence in a Heterogeneous Forest Using 3-D Radiative Transfer Modelling and Airborne LiDAR. *ISPRS J. Photogramm. Remote Sens.* **2022**, *191*, 1–17. https://doi.org/10.1016/J.ISPRSJPRS.2022.07.004.
2. Maes, W.H.; Pagán, B.R.; Martens, B.; Gentine, P.; Guanter, L.; Steppe, K.; Verhoest, N.E.C.; Dorigo, W.; Li, X.; Xiao, J.; et al. Sun-Induced Fluorescence Closely Linked to Ecosystem Transpiration as Evidenced by Satellite Data and Radiative Transfer Models. *Remote Sens. Environ.* **2020**, *249*, 112030. https://doi.org/10.1016/j.rse.2020.112030.
3. Ma, X.; Huete, A.; Moore, C.E.; Cleverly, J.; Hutley, L.B.; Beringer, J.; Leng, S.; Xie, Z.; Yu, Q.; Eamus, D. Spatiotemporal Partitioning of Savanna Plant Functional Type Productivity along NATT. *Remote Sens. Environ.* **2020**, *246*, 111855.
4. Zhuang, W.; Shi, H.; Ma, X.; Cleverly, J.; Beringer, J.; Zhang, Y.; He, J.; Eamus, D.; Yu, Q. Improving Estimation of Seasonal Evapotranspiration in Australian Tropical Savannas Using a Flexible Drought Index. *Agric. For. Meteorol.* **2020**, *295*, 108203. https://doi.org/10.1016/J.AGRFORMET.2020.108203.
5. Verrelst, J.; Rivera, J.P.; van der Tol, C.; Magnani, F.; Mohammed, G.; Moreno, J. Global sensitivity analysis of the SCOPE model: What drives simulated canopy-leaving sun-induced fluorescence? *Remote Sens. Environ.* **2015**, *166*, 8–21. https://doi.org/10.1016/j.rse.2015.06.002.
6. Gitelson, A.A.; Vina, A.; Ciganda, V.; Rundquist, D.C.; Arkebauer, T.J. Remote estimation of canopy chlorophyll content in crops. *Geophys. Res. Lett.* **2005**, *32*, 8.